JOURNAL OF SOLID STATE CHEMISTRY 65, 45–62 (1986)

X-Ray Diffraction and Electron Microscope Study of the Bi_2S_3–$PbBi_2S_4$ System

R. J. D. TILLEY

Department of Metallurgy and Materials Science, University College, Newport Road, Cardiff CF2 1TA, United Kingdom

AND A. C. WRIGHT

Department of Chemistry, UMIST, P.O. Box 88, Manchester M60 1QD, United Kingdom

Received December 11, 1985

An electron microscope and X-ray diffraction phase analytical study of the Bi_2S_3–galenobismutite (~$PbBi_2S_4$) system has been made on samples rapidly quenched from the melt and samples prepared by sintering Bi_2S_3 and PbS at a temperature of 996 K, 10 K below the eutectic temperature. Five well-ordered phases were found, Bi_2S_3, galenobismutite, and three twinned phases, V-1, V-2, and V-3. The X-ray powder data of these materials are given as well as the refined lattice parameters. Electron microscope examination of the samples using a technique involving slight misalignment of the crystal fragments allowed the structures of disordered materials in the phase V region to be determined.

Introduction

The structural way in which materials accomodate changes in anion-to-cation ratio is of interest, both from the viewpoint of the theoretical understanding of nonstoichiometric phases and experimentally, because such variations in atom ratios often produce significant changes in physical properties. One group of compounds which is of particular interest in this respect is that with structures which utilize twin planes to accomodate this change in composition. Such phases are referred to as chemically twinned (*1*).

The present paper reports upon an X-ray diffraction and transmission electron microscope study of some chemically twinned phases in the Bi_2S_3-rich region of the Bi_2S_3–PbS system. The aim of the study was to characterize both the ordered and disordered materials present using X-ray diffraction and electron microscopy so as to clarify this poorly characterized part of the phase diagram. In addition the results also provide data for theoretical studies of these nonstoichiometric compounds. The results of the study, reported in this paper, show that the disordered phases can be characterized using medium resolution electron microscope images and that a number of previously unreported structures exist in the phase region.

Previous Studies

The earliest noteworthy phase study of the PbS–Bi_2S_3 system, by van Hook (*2*),

0022-4596/86 $3.00

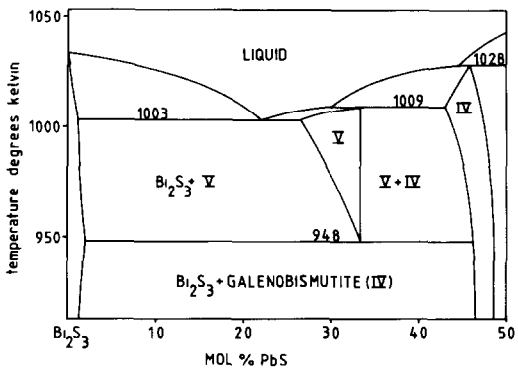

FIG. 1. The Bi_2S_3–$PbBi_2S_4$ region of the Bi_2S_3–PbS phase diagram, after Salanci and Moh (*4*).

did not reveal the presence of any high-temperature phases in the composition range between Bi_2S_3 and the phase galenobismutite, of approximate composition $PbBi_2S_4$. Both of these latter phases were reported as possessing no composition range. Since then two subsequent studies have recorded that at least one high-temperature phase does occur within this composition range. The study of Craig (*3*) indicated the presence of a line phase occurring at a composition of 35 mole% PbS and stable from 978 ± 5 to 1028 ± 5 K. In the most recent study, made by Salanci and Moh (*4*), the phase was reported as having an extensive composition range varying from 33.5 to 28.5 mole% PbS at the eutectic temperature of 1003 K. The stability range was given as 973 ± 5 to 1034 ± 2 K. In addition, Salanci and Moh noted that the X-ray powder patterns from the phase could be separated into those from PbS-rich and Bi_2S_3-rich samples, thus suggesting that the phase consisted of more than one compound. The phase diagram proposed by Salanci and Moh is shown in Fig. 1. On this diagram these high-temperature phases were designated by the Roman numeral V (five), a terminology that has persisted in later studies.

In regard to the phases Bi_2S_3 and galenobismutite, Salanci and Moh have suggested that there is negligible solubility of PbS in Bi_2S_3. Galenobismutite, on the other hand, was found to be somewhat Bi_2S_3 rich as indicated in Fig. 1.

The complexity of the structures in the phase V region was confirmed by Takéuchi and co-workers (*5*, *6*). The simplest structure, designated V-1 can be regarded as a member of the pavonite group of minerals found in the closely related Ag_2S–Bi_2S_3 system. It consists of two strips built of pairs of octahedra, shown as polyhedral outlines in Fig. 2a. These two sorts of strips have been designated as *A* and *B* type, respectively. The two strips, *A* and *B*, are linked by corner sharing of octahedra, so that phase V-1 can be represented by the sequence . . . *ABAB* . . . The spaces between the slabs generate square pyramidal sulfur coordination polyhedra, which contain metal atoms shown as circlces in Fig. 2a. The composition of V-1 is $PbBi_4S_7$, the Pb atoms occupying the octahedra of the *A* strips and Bi the octahedra of the *B* slabs and the square pyramids.

Two other phases were also characterised by Takéuchi, V-2, $Pb_2Bi_6S_{11}$, and V-3, $Pb_5Bi_{21}S_{36}$. Both of these structures can be formally derived from that of V-1 by the incorporation of twin planes, as shown in Figs. 2b and c. The twin planes only occur between the thicker *B* slabs and not the thinner *A* slabs, and V-2 and V-3 differ only in the separation of these twin planes. Formally we can represent the phases as

V-1 . . . ABAB . . .

V-2 . . . *BAB*BAB* . . .

V-3 . . . *BABAB*BABAB* . . .

where the asterisks represent twin planes. If twinning is limited to *B* slabs, as above, then V-1 represents a case of least twinning and V-2 the maximum amount of twinning possible. They are thus end members of a homologous series of compounds and V-3 is one of the many intermediate phases

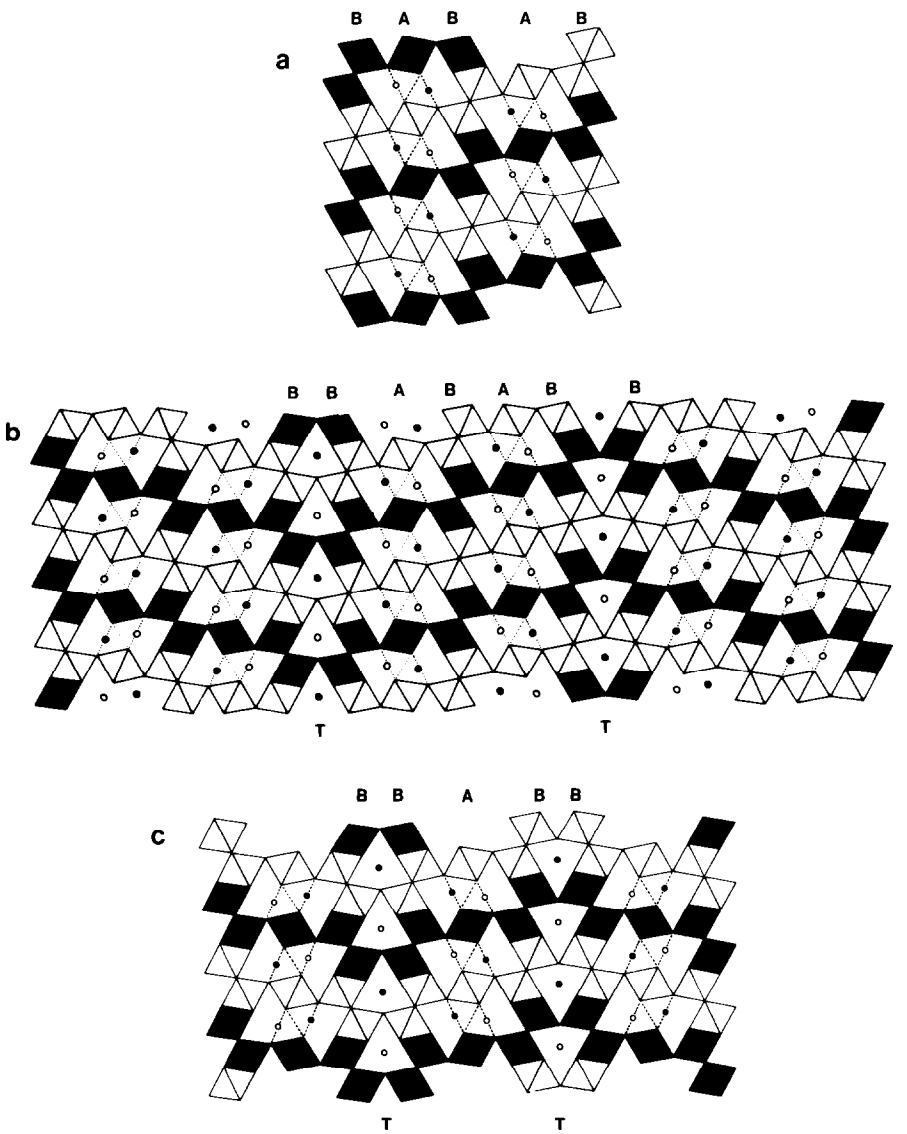

FIG. 2. Structures of the phase V group projected onto (001). (a) V-1, showing a regular alternation of *A* and *B* type slabs of two different widths. (b) V-3 and (c) V-2 are seen to be twinned variants of V-1. The twin planes, *T*, occur only between the thicker *B* slabs. The filled and open diamonds represent MS_6 octahedra at two different heights and the filled and open circles represent metal atoms at two different heights.

which can be constructed by the regular insertion of twin planes.

An electron microscope study of the PbS–Bi_2S_3 system be Colaïtis *et al.* (*7*) included the phase V region. Much of the emphasis was in the interpretation of diffraction patterns using techniques of general validity for twinned materials (*8*). Because of this, studies focused largely upon ordered strutures. Two new sequences of twins were observed, giving rise to phases V-4 and V-5, with structures

V-4 . . . *BABABAB* . . .

V-5 . . . *BABABABAB* . . .

Several regular intergrowths of the phases V-2 with V-3, and V-3 with V-4 are also mentioned.

The structures of all of these phases can be derived from that of a parent material with the *galena* (PbS) structure, which is similar to that of NaCl (*7–10*). For the phase V group, the *A* and *B* slabs can be regarded as thin slices of *galena* cut parallel to (311). Figure 3 shows this structure and its relationship to the phase V compounds. The relationships between the structures of *galena*, Bi_2S_3, and galenobismutite are less easy to see, but both these latter phases can also be derived from the regular insertion of (311) twins into *galena* together with a modulation of the atomic positions along the twin boundaries. The diffraction geometry of all the phases is therefore closely linked to that of *galena* periodically twinned on (311) planes (*8*).

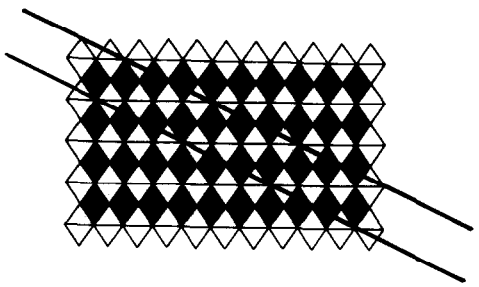

FIG. 3. The structure of PbS projected onto (110). The filled and open diamonds represent MS_6 octahedra at two different levels. The projection of two (311) planes marked on the diagram as heavy lines, delineate the *B* slab width in the phase V structures.

Experimental

Materials

All samples prepared in this study were produced from high-purity lead, bismuth, and sulfur. These chemicals were supplied by Johnson Matthey Ltd. and were of Specpure grade. The total metallic impurity content of each chemical was determined by the suppliers not to exceed 10 ppm. The lead rods were heavily tarnished and so the surface was scraped away by the use of a fresh surgical scalpel. Small pieces of lead were then cut off with a clean pair of electrician's side cutters. Smaller chips were pared away with a scalpel. The large bismuth lumps were broken down to smaller pieces by the combined use of a punch and a percussion mortar. Sulfur was received as a fine powder and required no further treatment. The lead and bismuth had a tendency to tarnish after a few weeks even when kept in closed vessels and so fresh material was prepared when new samples were required.

Preparation

Samples examined in this study were prepared in one of two ways. Four samples were prepared by melting mixtures of the elements and then quenching the molten material into iced brine. The compositions prepared were 20, 25, 30, and 35 mole% PbS. A more extensive series of samples was prepared by sintering mixtures of PbS and Bi_2S_3. These latter compounds were prepared by direct fusion of 20-g quantities of the elements and were checked for purity by powder X-ray diffraction after synthesis. Appropriate weights of the PbS and Bi_2S_3 so prepared were ground together in an agate mortar before being pressed into pellets. The compositions prepared covered the range from 26 mole% PbS to 50 mole% PbS in 1 mole% steps. Additional samples with compositions of 10 and 20 mole% PbS were also prepared. These were sintered for 3 days at 998 K, which was about 10 K below the eutectic temperature.

All samples were reacted in sealed, evacuated, silica ampoules. For the sintered samples it was important to maintain a

careful control of the temperature to prevent partial melting of the materials. To prevent this, the ampoules were placed in holes drilled in a massive nickel alloy cylinder which acted as thermal buffer. Temperature control of the cylinder and its samples was afforded in two steps. First, the platinum/rhodium thermocouple from the furnace control module was placed in direct contact with the cylinder and the high thermal mass of the cylinder acted so as to damp the control system. Second, the output from a second platinum/rhodium thermocouple, also placed in direct contact with the cylinder, was measured against an identical thermocouple, placed in iced water. In this way, the temperature of the samples was set to within ±2 K and monitored independently of the temperature control system.

Characterization

All samples were examined by X-ray powder diffraction using a Hägg-Guinier focusing camera employing strictly monochromatic Cu$K\alpha_1$ radiation and KCl (a_0 = 0.62923 nm at 298 K) as an internal standard. In many cases, several parts of each sample were X-rayed so as to account for any gross inhomogeneities that might have occurred. When necessary, films were measured against a scale printed on the film prior to processing so as to compensate for film shrinkage. The measurements were refined using least-squares procedures (*11, 12*) and indexed taking into account previous structural studies and anticipated line intensities. The relative intensities of reflections were measured from the films using a Joyce Loebl double beam recording microdensitometer taking the relative peak heights as a direct measure of the relative intensities.

Samples were examined in a JEM 100B electron microscope fitted with a double tilt top entry goniometer stage and operated at 100 kV. Electron microscope specimens were prepared by crushing selected crystals in an agate mortar under *n*-butanol and allowing a drop of the resultant suspension to dry on a holey carbon film supported on a copper grid. The crystals were imaged in standard ways after alignment so that the short crystallographic axis of the material was parallel to the electron beam. Further details are given in the following section.

Interpretation of Electron Microscope Data

Diffraction Patterns

The crystal structures of the phases Bi_2S_3 and galenobismutite are well known, and so the expected electron diffraction patterns can readily be generated. For positive identification, the most useful projection is that down the short (0.4 nm) cell axis, as in the diffraction patterns shown in Fig. 4.

The geometrical characteristics of the diffraction patterns generated by chemically twinned structures such as the phase V compounds have been analyzed by van Dyck *et al.* (*7, 8*) and Mackoviky (*10*). The analysis of diffraction patterns is of importance only when well-ordered materials are being considered. As much of the interest in the present study was centered upon disordered materials, the full analysis will not be described here.

The diffraction patterns recorded from the three different well-ordered phase V compounds prepared in these studies are shown in Figs. 4c, d, and e. They can be considered to be generated from the PbS diffraction pattern, and differ only in the existence of rows superstructure reflections parallel to g_{311} which result from the periodic array of (311) twin planes in the *galena* matrix. The intensity of the superstructure reflections is modulated and comes to a maximum in the vicinity of the PbS reciprocal lattice points. The spot spacing along any noncentral row of reflections gives the

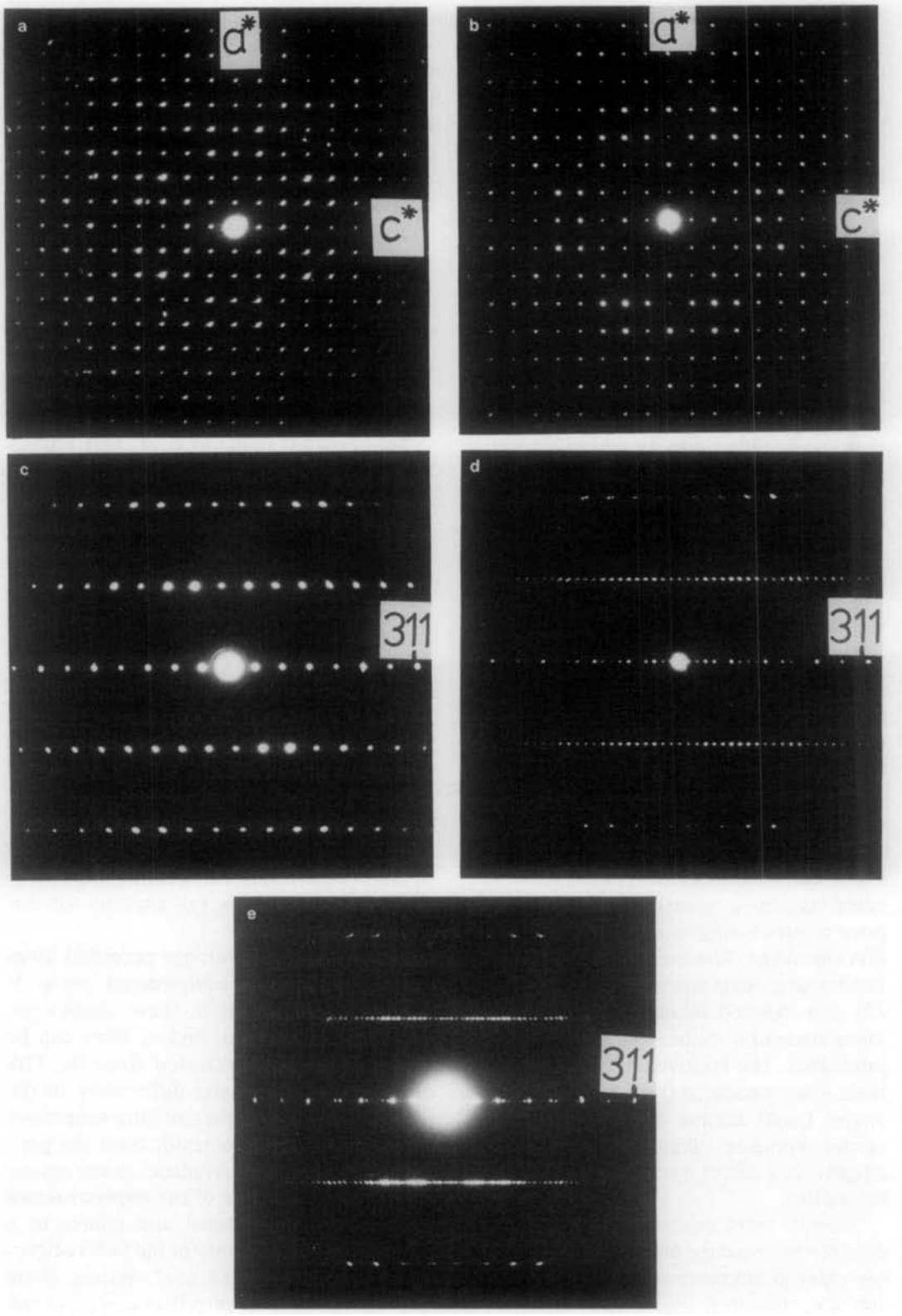
a
a*
c*
b
a*
c*
c
311
d
311
e
311

long axis periodicity directly. These values for the known phase V compounds are: V-1, 1.2 nm; V-2, 3.6 nm; and V-3, 6.0 nm.

Images

Identification of Bi_2S_3 and galenobismutite proved straightforward in view of the fact that the phases are normally well ordered and possess characteristic diffraction patterns. An analysis of image contrast is important, however, in the phase V region, as materials are very similar structurally and frequently disordered.

The electron microscope used in the present study did not have a sufficiently high resolution to produce images which revealed directly the atom positions in the phases, even for thin, well-aligned crystal fragments. However, when such fragments are imaged under certain conditions of slight misalignment, the images of the known phase V compounds were found to contain full information on the stacking sequence of the type *A* and type *B* PbS slabs. Because of the considerable usefulness of the technique it is described.

If a twinned crystal is imaged so that the twin plane is parallel to the electron beam, both parts of the crystal will appear to have identical contrast, and only a weak contrast will arise at the boundary twin plane. By slight misalignment, however, it is possible to create diffraction conditions whereby only one of the two twin orientations is diffracting strongly. In such a case, one twin region would appear black and the other white on a normal micrograph. The twin plane is found at the boundary between the two regions.

The same effect is found in phases built of regular sequences of twinned slabs. Consider the case where the twinned slabs are fairly wide, and of equal width, such as in the mineral phase heyrovskyite $Pb_6Bi_2S_9$ (*7, 9*). When the twin planes are exactly parallel to the electron beam, the only visible contrast will arise from the twin planes themselves when the image is formed from the central systematic row of reflections. If the crystal is slightly misaligned a new intensity pattern can be seen. Under the best conditions only one of the two twin orientations is diffracting strongly. Thus one sees alternate light and dark strips of contrast. The width of each strip corresponds to the width of a twin slab and the twin planes will then be at the interface between the light and dark strips. If diffracted beams from more than one systematic row are included then two dimensional fringe patterns are produced. The two types of bright fringe are still visible under these conditions but less easy to recognise.

In the case of the phase V structures we have two twin effects combined. Reference to Fig. 2 shows that the *A* and *B* type slabs are in a twin relationship to each other. They are also considerably thinner than in the cases described above. Imaging phase V-1, would therefore produce a set of broader bright fringes corresponding to *B* slabs separated by narrower black fringes corresponding the *A* slabs. Slight reorientation of the crystal should then reverse the contrast to produce broader dark fringes corresponding to the *B* slabs and narrower bright fringes corresponding to the *A* type slabs.

When a more complex structure, such as the phase V-3 is considered, we now have the added complication of the superposition of a further twin plane into the structure.

FIG. 4. Electron diffraction patterns of (a) Bi_2S_3, (b) galenobismutite, (c) V-1, (d) V-2, and (e) V-3. In (a) and (b) the a^* and c^* axes are marked. In (c), (d), and (e), the b^* axis lies along the direction of the closely spaced superlattice spots. The superstructure reflection corresponding to the *galena* 311 reflection is marked.

This will have the expected consequences so that as one traverses this second twin plane, the contrast effects will be reversed. Let us consider this in more detail. The stacking sequence of the V-3 structure is given by

. . . B*B A B A B*B A B A B*B A B A B* B . . .

The twin planes are marked by asterisks and the repeat periodicity encompasses the material between every alternate twin plane as shown. This is because adjacent twin planes are of "opposite sense" and so the periodicity will always be double the twin plane spacing for any twinned phase. If diffraction conditions are such that twin slabs of only one orientation are now visible then the resulting pattern of broad and narrow bright fringes will be

. . . B*BABAB* BABA B* BABAB*B . . .
| | | | | | | | |
b b b n n b b b

where *b* is a broader, more intense bright fringe and *n* a narrower less intense bright fringe. Thus a unit cell image will contain three broad and intense bright fringes followed by two narrower and less intense bright fringes. A slight change in crystal orientation will reverse the contrast and give the complete stacking sequence from the image fringe pattern.

To illustrate the use of the technique with an unknown structure, suppose that a periodic sequence of three broad and three narrow bright fringes are observed. This can be written as

. . . B—B—B—A—A—A . . .

From the positions of the dark fringes, and our knowledge of how the contrast changes on passing a twin plane we can insert twin planes thus:

. . . *B—B—B—*A—A—A* . . .

where the asterisks represent the twin planes, and so generate the whole stacking sequence:

. . . *BABABA*ABABAB* . . .

If the fragment is tilted in the opposite sense, then the other set of twin slabs will produce intense fringes so that for the above example, we will have, from left to right, three narrow fringes and three broad fringes. Working through the same procedure will give us exactly the same stacking sequence. By taking the thickness of the *A* and *B* type PbS slabs from known structures the periodicity of the new structure can be estimated quite accurately.

The above analysis assumes that the phases are chemically twinned with even numbers of a given type of PbS slab in a group. If this assumption does not hold then it is not possible to find the stacking sequence from only one image. Fringe patterns will then have to be recorded with one set of twin slabs diffracting and then with the other set by reversing the tilt on the fragment. By comparing the two fringe patterns over the same area, it will then be possible to deduce the stacking sequence.

Although the method of interpretation does not take into account complex diffraction effects its usefulness stems from its ability to interpret correctly the fringe patterns of phases for which the detailed stacking sequence is known, such as for V-3, and its ready extension to disordered materials. Moreover it can be seen that the atomic resolution is not necessary in order to characterize the nature of such twinned phases, all that is needed is the ability to resolve the individual rocksalt slabs which are spaced approximately 0.6 nm apart. For this purpose, the images need only be formed from diffracted 0*k*0 beams out to at least 1.67 nm^{-1}. Relatively low magnification can be used, thus giving higher contrast images and larger areas of crystal to consider. This is of great assistance when working on beam sensitive materials.

TABLE I

X-RAY PHASE ANALYSIS OF Bi_2S_3–$PbBi_2S_4$

Mole% PbS	Phases Present
10	Bi_2S_3 + small amount of unidentified material
20	Approximately 50/50 Bi_2S_3 and V-1
26	Mostly V-1 plus some Bi_2S_3
27	Fairly pure V-1
28	Bi_2S_3 + V-1 + V-3
29	Mostly Bi_2S_3 plus some galenobismutite and Bi_2S_3
30	Bi_2S_3 + V-3 + galenobismutite
31	Mostly V-3 plus some Bi_2S_3 and galenobismutite
32	V-3 + Bi_2S_3 + galenobismutite } Plus a very faint trace of Bi_2S_3
33	V-3 + Bi_2S_3 + galenobismutite
34	V-3 + Bi_2S_3 + galenobismutite
35	V-3 + Bi_2S_3 + galenobismutite
36	Mixture of V-3 and galenobismutite. Possibly a trace of Bi_2S_3
37	V-3 plus galenobismutite
38	V-3 plus galenobismutite
39	V-3 plus galenobismutite
40	V-3 plus galenobismutite
41	V-3 plus galenobismutite
42	V-3 plus galenobismutite
43	V-3 plus galenobismutite
44	V-3 plus galenobismutite
45	V-3 plus galenobismutite
46	V-3 plus galenobismutite
47	V-3 plus galenobismutite
48	V-3 plus galenobismutite
49	V-3 plus galenobismutite
50	Fairly pure galenobismutite plus a trace of V-3

Results

X-Ray Phase Analysis

A. Sintered material. In the series of samples which were prepared by the reaction of Bi_2S_3 and PbS at 998 K, three phases were unequivocally identified in addition to Bi_2S_3. In increasing PbS content they are: V-1, V-3, and galenobismutite $PbBi_2S_4$. A fourth phase was observed in a sample containing only 10 mole% PbS. This was not positively identified but is probably a disordered phase V compound. No trace of the V-2 phase was found.

Fairly pure V-1 was found in material containing 27 mole% PbS which corresponds to a composition of $MS_{1.422}$. This is in fair agreement with the experimental lower PbS limit of the phase V range quoted by Salanci and Moh (*4*) as 26 mole% PbS or $MS_{1.425}$. Purest V-3 was found in material containing 31 mole% PbS giving a composition of $MS_{1.408}$ which is only in fair agreement with the value of 33.6 mole% PbS, $MS_{1.399}$ calculated by Takéuchi (*6*). No lattice parameter shifts or solid solution ranges were observed in this series of samples. The powder X-ray phase analysis for the series is given in Table I.

B. Melt quenched material. Despite the rapid freezing of these samples, their X-ray powder patterns showed relatively well-ordered phases. The phases found were: V-1, V-2, and galenobismutite. No trace of V-3

could be found. Purest V-2 was found in the sample containing 30 mole% PbS giving a stoichiometry of $MS_{1.412}$. This agrees reasonably well with that calculated by Takéuchi (*6*) as 30.7 mole% PbS, $MS_{1.409}$. Purest V-1 was found in the sample containing 25 mole% PbS or $MS_{1.429}$. Since these materials will obviously be nonequilibrium, little significance can be attached to analysis of their compositions.

There was no obvious evidence for the formation of new phases in these samples. No lattice parameter shifts or solid solution ranges were observed. The powder X-ray phase anlaysis of these preparations is given in Table II.

C. Lattice parameter refinement. Despite the fact that the X-ray films were complex, as no strictly monophasic preparations were obtained, it was found possible, by careful comparison of many X-ray powder patterns, to separate those reflections belonging to each known phase V compound. Where reflections overlapped, as they often did, they were identified by observing the change in intensity with composition. In this way, no reflections were left out due to uncertainty in their origin, and all three of the phase V unit cells could be refined. No experimental powder patterns are available for comparison. A theoretical pattern for the V-1 phase as derived from the known structure is shown in Fig. 5 (*5*). In terms of the *d* values this compares reasonably well with a densitometer trace of a V-1 powder pattern obtained in this study also shown in Fig. 5 although there are considerable differences in the relative intensities between the two sets of data. No densitometer traces are given for V-2 and V-3 because powder patterns of sufficiently pure phases were not obtained. Indexed *d* values for V-1, V-2, and V-3 are given in Tables III, IV, V.

The X-ray diffraction patterns of the phases Bi_2S_3 and galenobismutite were analyzed by reference to the ASTM data (*13,*

TABLE II

X-RAY PHASE ANALYSIS OF Bi_2S_3–$PbBi_2S_4$ MELT QUENCHED SAMPLES

Mole% PbS	Phases Present
20	Mixture of Bi_2S_3 and V-1. Some reflections slightly diffuse
25	V-1 plus a faint trace of Bi_2S_3
30	V-2 plus a faint trace of Bi_2S_3
35	V-2 plus galenobismutite

TABLE III

X-RAY POWDER DATA FOR V-1, $PbBi_4S_7$

	Present study		Takéuchi (*5*)	
d_{obs} (nm)	Visual intensity	*hkl*	d_{cal}	Calculated intensity
0.5783	W	020	0.5815	19
0.5070	VW	210	0.5077	7
0.4974	W	$\bar{2}20$	0.4995	9
0.3846	M	101	0.3844	100
0.3827	M	220	0.3837	—
0.3783	M	$\bar{2}30$	0.3778	76
0.3766	M	111	0.3737	13
0.3563	M	$\bar{1}11$	0.3568	44
0.3323	M	$\bar{1}21$	0.3328	35
0.3307	M	$\bar{4}10$	0.3311	41
0.3194	VW	400	0.3199	2
0.2968	S	$\bar{3}11$	0.2968	63
0.2926	M	301	0.2929	19
0.2837	VW	$\bar{1}31$	0.2842	15
0.2823	M	$\bar{3}21$	0.2826	41
0.2726	M	311	0.2728	37
0.2561	W	$\bar{3}31$	0.2567	8
0.2415	VW	240	0.2421	6
0.2404	W	$\bar{1}41$	0.2411	13
0.2387	W	$\bar{2}50$	0.2394	10
0.2317	W	050	0.2326	14
0.2232	M	141	0.2237	34
0.2147	M	600	0.2132	5
0.2043	M	511	0.2045	17
0.2014	M	002	0.2015	22
0.2005	W	$\bar{2}60$	0.2005	15
0.1999	W	$\bar{3}51$	0.2004	—
0.1978	M	$\bar{6}40$	0.19818	11
0.1945	M	$\bar{5}41$	0.19503	19
0.1783	M	222	0.17839	13
0.1777	M	$\bar{2}32$	0.17779	12
0.1731	W	531	0.17327	—
0.1720	M	$\bar{2}70$	0.17203	—
0.1709	W	$\bar{7}21$	0.17107	7

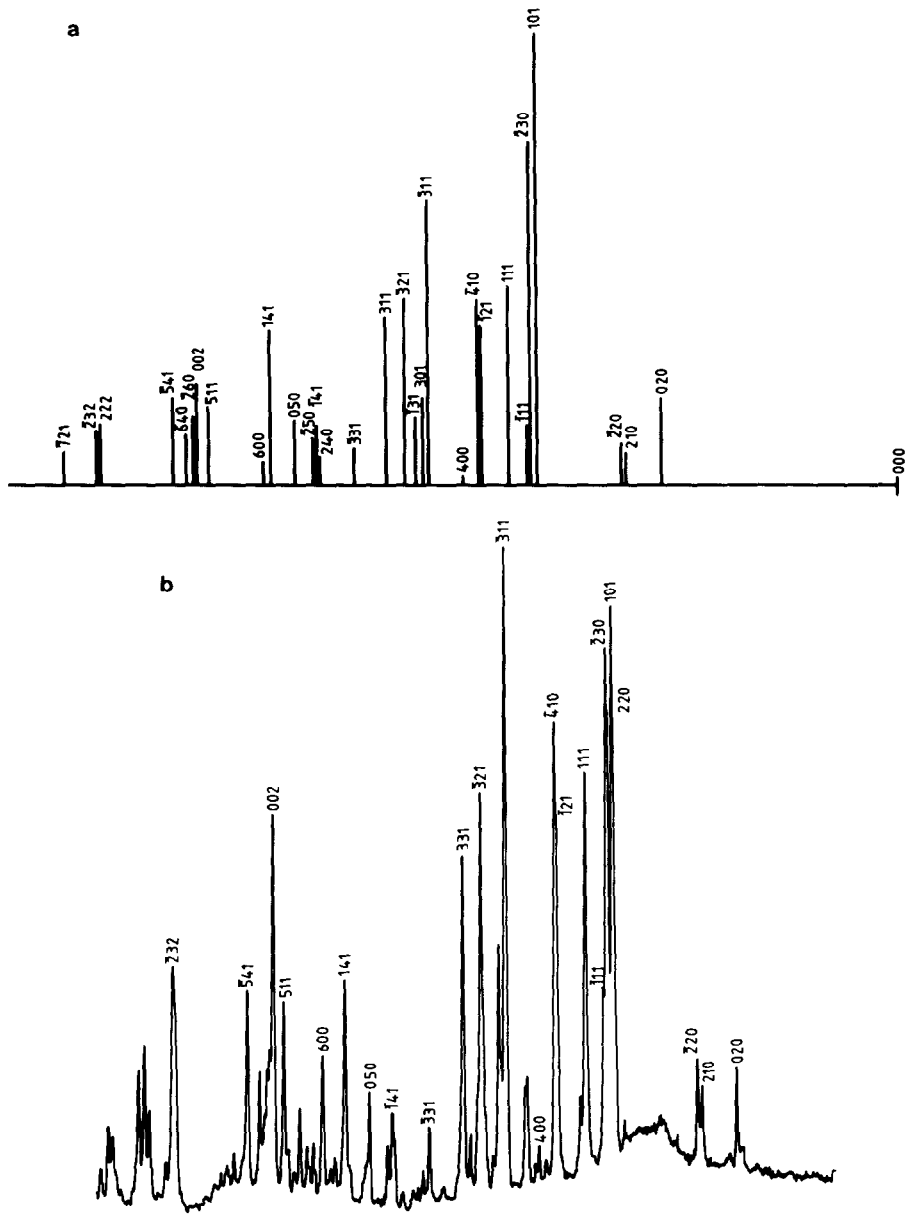

FIG. 5. (a) Calculated X-ray powder pattern of phase V-1 (*4*). (b) Experimental X-ray powder pattern of V-1.

14). As the X-ray patterns obtained in this study contain more reflections than those listed in the ASTM index we reproduce our data in Tables VI and VII.

The lattice parameters of the five well-ordered phases found are listed in Table VIII along with previous literature values. It can be seen that there are no major discrepancies between the figures.

Electron Microscopy

Crystal fragments of both Bi_2S_3 and gale-

TABLE IV

X-RAY POWDER DATA FOR V-2, $Pb_2Bi_6S_{11}$

d_{obs} (nm)	Visual intensity	*hkl*
0.6099	W	060
0.4911	M	170
0.3861	W	111
0.3816	W	350
0.3768	VS	280
0.3682	M	131
0.3419	M	151
0.3308	S	400
0.3267	M	420
0.3190	W	241
0.2979	W	261
0.2967	M	311
0.2942	M	460
0.2893	M	331
0.2832	W	191
0.2799	W	351
0.2758	S	281
0.2679	W	510
0.2435	W	391
0.2291	W	461
0.2178	W	531
0.2167	W	640
0.2111	W	551
0.2082	M	660
0.2021	S	002
0.1987	M	112
0.1946	M	591
0.1895	W	710
0.1884	W	242
0.1782	S	352
0.1725	M	402

nobismutite were found to be well ordered, and will not be considered further here. Most interest centred upon the disordered phase V region, which presents problems of interpretation. In this section we show only three examples of electron micrographs of disordered materials, to illustrate the use of wider and narrower bright fringes in determining the sequence of *A* and *B* layers. It must be noted that any one individual micrograph may not give a completely unequivocal answer, but slight changes in the degree of misalignment of the crystal can usually resolve any uncertainties. In addition, the images shown were formed by allowing extra diffracted beams in addition to those from the central row of systematics to fall within the objective aperture to produce the two-dimensional fringe patterns visible. The images were recorded under conditions of slight misalignment, however, and show the broad and narrow bright fringes as described in the previous section, thus enabling interpretation to be made. Note, how-

TABLE V

X-RAY POWDER DATA FOR V-3, $Pb_3Bi_{10}S_{18}$

d_{obs} (nm)	Visual intensity	*hkl*
0.6044	W	240
0.5002	W	280
0.3857	W	111
0.3796	VS	131
0.3746	W	061
0.3675	W	151
P.3601	W	081
0.3526	W	171
0.3456	M	201
0.3434	W	221
0.3399	W	241
0.3338	M	400
0.3317	M	420
0.3244	W	440
0.3195	W	460
0.3008	W	480
0.2975	M	311
0.2945	VW	331
0.2920	W	351
0.2867	W	371
0.2766	W	391
0.2717	VW	510
0.2421	W	481
0.2172	W	660
0.2157	W	571
0.2115	S	591
0.2073	M	002
0.2009	W	042
0.1987	W	132
0.1931	W	641
0.1886	W	681
0.1773	S	392
0.1715	M	442
0.1705	W	751
0.1666	W	820
0.1651	W	860
0.1636	W	880

TABLE VI

X-RAY POWDER DATA FOR Bi_2S_3

Present study			ASTM, Swanson (14)		
d_{obs} (nm)	Visual intensity	*hkl*	d_{obs} (nm)	Visual intensity	*hkl*
0.7915	W	101			
0.5643	M	200	0.565	20	020
0.5562	M	002			
0.5036	M	201	0.504	19	120
0.4988	M	102			
0.3963	S	202	0.397	38	220
0.3743	S	011	0.375	20	101
0.3564	S	301	0.356	94	130
0.3549	S	111			
0.3523	VS	103	0.353	60	310
0.3249	M	201	0.3256	18	021
0.3120	VS	302	0.3118	100	230
0.3109	VS	203			
0.2805	VS	213	0.2811	63	221
0.2711	S	013	0.2716	34	301
0.2701	W	104			
0.2636	M	011	0.264	24	311
0.2515	M	402	0.252	35	240
0.2494	M	204	0.2499	13	420
0.2450	M	213	0.2456	15	231
0.2298	M	410	0.2304	24	041
0.2251	M	403	0.2256	36	141
0.2233	M	114			
0.2198	VW	313			
0.2182	W	105			
0.2123	W	412	0.2129	9	241
0.2112	M	214	0.2118	15	421
0.2088	W	502	0.2096	11	250
0.2070	M	205	0.2074	10	520
0.1986	S	404	0.199	33	002
0.1979	W	413			
0.1947	S	015	0.1953	55	431
0.1940	S	511	0.1935	20	151
0.1931	W	121			
0.1926	W	305			
0.1913	M	115	0.1919	20	530
0.1878	W	220	0.1884	14	060
0.1871	VW	022			
0.1853	W	221	0.1854	17	251
0.1847	VW	215			
0.1826	M	106	0.1834	7	610
0.1774	M	414	0.1779	13	222
0.1761	W	206	0.1765	5	620
0.1746	VW	513	0.1737	7	351
0.1734	S	123	0.1734	35	312
0.1729	S	315			
0.1698	W	610	0.1703	10	061
0.1662	W	116	0.1682	7	161

ever, that where misalignment is used to form the desired two fringe pattern, there seems to be an optimum crystal thickness where the bright fringes are most visible.

TABLE VII

X-RAY POWDER DATA FOR GALENOBISMUTITE, $PbBi_2S_4$

Present study			ASTM, Berry (13)		
d_{obs} (nm)	Visual intensity	*hkl*	d_{obs} (nm)	Intensity	*hkl*
0.7243	VW	002			
0.4567	M	202	0.455	10	220
0.4476	W	201			
0.3909	M	011	0.393	5	011
0.3629	S	004	0.365	30	040
0.3468	M	104			
0.3450	VS	302	0.345	100	320
0.3395	S	112			
0.3342	S	210	0.336	5	201
0.3255	M	211	0.327	5	211
0.3009	S	113	0.303	40	131
0.2879	VW	401			
0.2767	M	213	0.276	30	311
0.2750	M	402			
0.2725	M	304			
0.2637	M	312	0.265	20	141
0.2513	W	403			
0.2459	S	313	0.246	40	241
0.2437	W	006			
0.2381	M	106	0.239	20	401
0.2263	W	412			
0.2237	M	314	0.224	10	421
0.2192	M	215	0.220	10	251
0.2059	M	116			
0.2047	M	020	0.205	40	360
0.2031	M	315			
0.2016	M	511	0.201	5	511
0.1991	M	121			
0.1960	S	600	0.1961	50	261
0.1876	W	406	0.1881	20	531
0.1868	W	123			
0.1840	W	307	0.1848	5	—
0.1824	W	008			
0.1816	W	603			
0.1793	M	223	0.1784	5	—
0.1772	M	217	0.1762	30	—
0.17504	S	611			
0.1725	M	604	0.1734	10	—
0.1698	W	506	0.1704	5	—

TABLE VIII

LATTICE PARAMETERS OF THE PHASE V MATERIALS[a]

Galenobismutite: ($PbBi_2S_4$)	Present study	a = 1.1753	b = 0.4087	c = 1.4612	
	Previous value (*16*)	a = 1.1790	b = 1.4590	c = 0.4100	
V-2:	Present study	a = 1.3278	b = 3.6768	c = 0.4034	
	Previous value (*5*)	a = 1.33	b = 3.68	c = 0.403	
V-3:	Present study	a = 1.3366	b = 5.9542	c = 0.4060	
	Previous value (*5*)	a = 1.3343	b = 6.0022	c = 0.4033	
V-1:	Present study	a = 1.3461	b = 1.2371	c = 0.4028	γ = 99.19°
	Previous value (*5*)	a = 1.3247	b = 1.2042	c = 0.4030	γ = 105.02°
Bi_2S_3:	Present study	a = 1.1334	b = 0.3957	c = 1.1144	
	Previous value (*17*)	a = 1.111	b = 1.125	c = 0.397	

[a] Values in nanometers.

This may be related to the first extinction distance where the intensity of the diffracted beams reach a maximum. Also, of course, the focus will vary slightly over the fragment, so that sequence identification will always be optimum in rather precise regions of crystal.

Figures 6a and b are from a sample of overall composition 30 molc% PbS: 70 mole% Bi_2S_3 quenched from the melt. Figure 6a shows three different b periodicities and fringe patterns, two of which represent the phases V-1 and V-2. The third represents a new sequence . . . B*B A B A A A A B A B*B . . . Figure 6b also shows the fringe patterns and periodicities of V-1 and V-2 but with the new stacking sequences of . . . B*B A B A A B A B*B . . . and

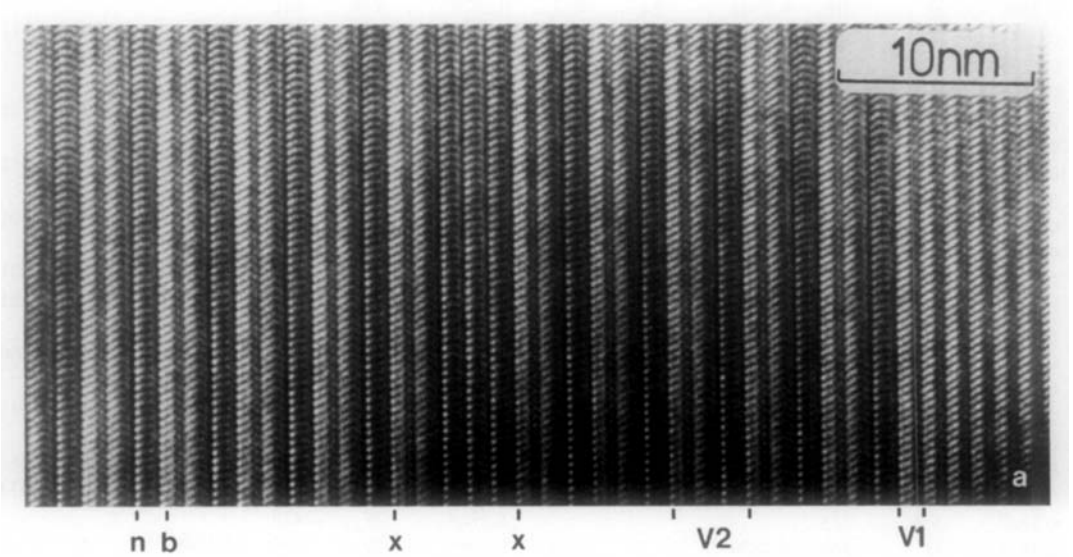

FIG. 6. Electron micrographs of disordered phase V crystals showing broad (b) and narrow (*n*) fringes. (a) The crystal contains areas of phases V-1, V-2, and the new sequence BABAAAABAB between *x* and *x*. (b) the crystal contains areas of phases V-1, V-a, and the new sequence BABAABAB between *x* and *x*. (c) Stacking sequences of (1) BABAAAAAABAB, (2) BABABABAAAABABA-BAB, (3) BABAAAAAABAB, (4) BABAAAABAB, (5) BABABAAAABABAB, and (6) BABABA-BABBBBBBABABABAB.

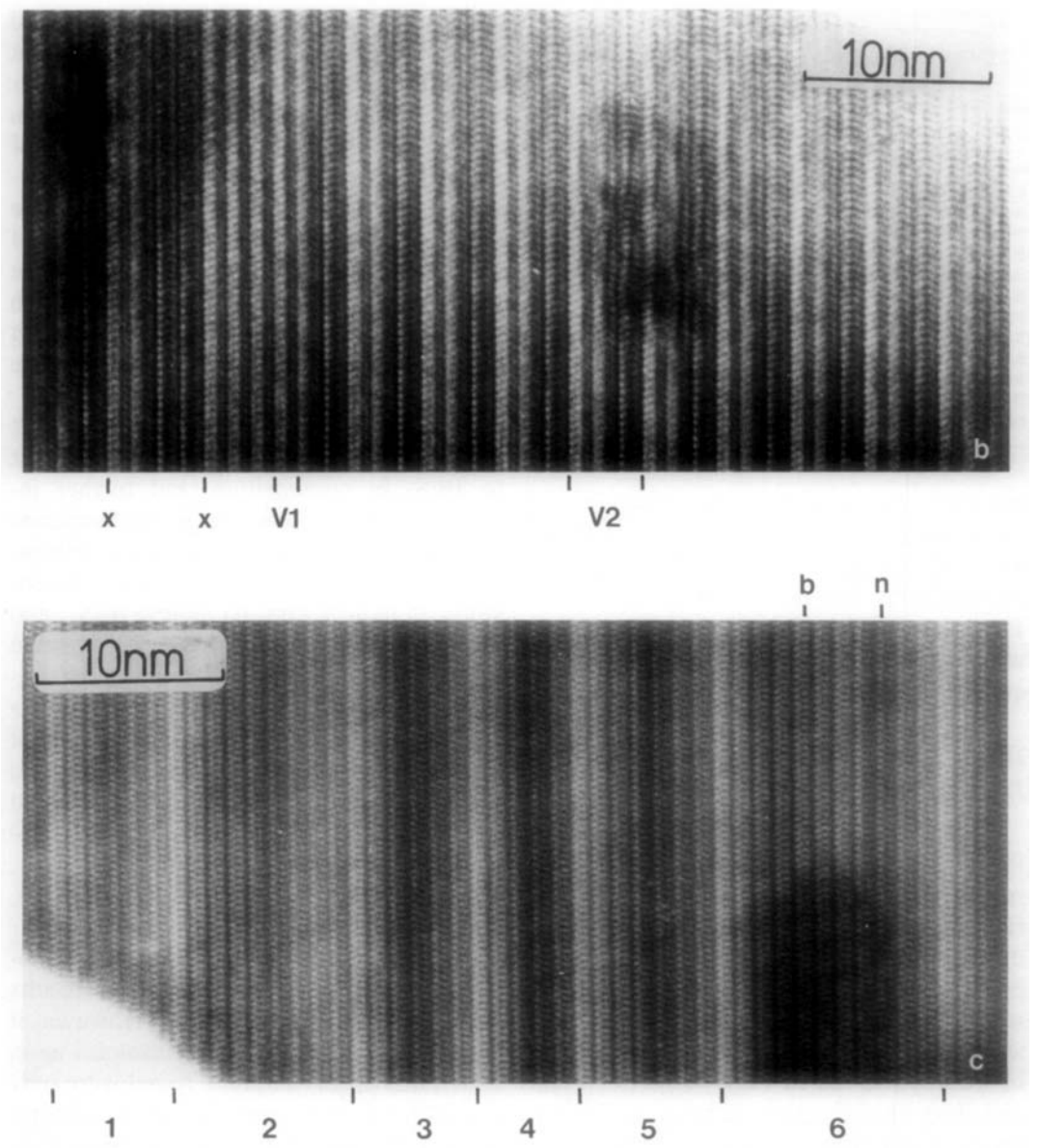

FIG. 6—*Continued.*

. . .B*B A A B*B . . . Figure 6c shows a highly disordered sequence of new periodicities, with values for *b* ranging from 5.6 to 13.3 nm. The image formed in this case is not easy to interpret but it is still possible to recognise the two types of fringe used for analysis. The images in Fig. 6 would have been easier to interpret had only beams from the central row been included within the objective aperture such that one-dimensional fringes were produced.

The electron microscope phase analysis showed the presence of the three phase V compounds and a variety of long period sequences not reported previously. It was noted that more of these new sequences

TABLE IX

STACKING SEQUENCE OBSERVED IN THE PHASE V REGION OF THE Bi_2S_3–PbS SYSTEM

Stacking sequence repeat	x in MS_x	b periodicity (nm)
BABBBBBBBBAB	1.353	7.646
BABBAB (V-2)	1.375	3.655
BABABBBBABAB	1.375	7.312
BABABABABBBBBB ABABABAB	1.353	13.294
BABABBABAB (V-3)	1.385	5.954
BAAB	1.400	2.326
BABAABAB	1.400	4.652
BABABAABABAB	1.400	6.978
BABABAAABABAB	1.412	7.974
BABAAAABAB	1.417	5.648
BABAAAAAABAB	1.429	6.644
BABABABAAAABABABAB	1.4375	10.300

were found in sintered samples than in materials quenched from the melt. A list of the new stacking sequences, together with their compositions are presented in Table IX. There is no doubt that if the examination were to be continued, further new sequences would be found.

Discussion

Phase Analysis

Although precise phase analysis was not the primary aim in the present study, results showed that five well-ordered materials were produced at the temperatures used, Bi_2S_3, galenobismutite, and the phases V-1, V-2, and V-3. Our experiments were not designed to reveal if Bi_2S_3 possessed a composition range, but electron microscopy revealed only perfect crystals and electron diffraction patterns, so that we can conclude that if Bi_2S_3 does form a nonstoichiometric phase by reaction with PbS it is structurally well ordered and possesses the Bi_2S_3 structure.

In samples sintered at approximately 10 K below the eutectic temperature, the phase in equilibrium with Bi_2S_3 is V-1. The addition of more PbS then produces phase V-3 before ultimately forming galenobismutite. As galenobismutite still existed together with a trace of phase V-3 when the overall composition of the samples were 50 mole% PbS: 50 mole% Bi_2S_3 it suggests that galenobismuthite has a composition closer to $PbBi_2S_4$ than that suggested by Salanchi and Moh (*4*). The X-ray powder patterns of all the phases in the composition range covered showed no systematic variation of line positions or intensities. While this is not of relevance for the Bi_2S_3 or galenobismutite phases, as these would be at their PbS-rich and Bi_2S_3-rich phase limits, respectively, it does indicate that V-1 and V-3 are line phases.

In the samples which were melt quenched, the phase V-1 was again nearest to Bi_2S_3 in composition, but further increase in PbS content lead to the formation of phase V-2. This phase coexisted with galenobismutite in samples of overall composition 35 mole% PbS: 65 mole% Bi_2S_3, and the phase V-3 did not appear. It is certain that these melt quenched samples are unlikely to consist of equilibrium phase assemblies, but despite this, a comparison of these results with those from the sintered preparations indicates that phases V-2 and V-3 may have different temperature domains of stability. The difference may, however, also reflect formation conditions, and as such is considered further below.

As far as the composition of the galenobismutite phase is concerned, our results indicate that it is not Bi_2S_3 rich. However, it is necessary to note that the samples upon which this observation are based were only heated for 3 days, and may not be in equilibrium. On the other hand, the firing temperature was only some 10 K below the eutectic temperature, and reaction would be expected to be rapid under these conditions. Moreover, the X-ray technique used in our studies is capable of detecting very small amounts of phases such as V-2 and V-3. A less sensitive method may not detect these compounds, and so could give the impression that the phase was rich in Bi_2S_3. Clearly more preparations at a variety of

heating times and temperatures are needed to clarify this point.

Formation of Phase V Stacking Sequences

The results reported here show that material quenched from the melt is largely well ordered, and the major products appear to be well formed V-1 and V-2. As mentioned above, these compounds are the end members of a series of phases, with V-1 being Bi_2S_3 rich and V-2 being PbS rich. In the melt we can assume that the Bi and Pb components are homogenously distributed, and hence on cooling the most stable phases would be expected to separate. It would appear that V-1 and V-2 are these stable phases.

The complexity that is found in the sintered samples is therefore representative of the solid state reaction. Unfortunately, our data give no information as to the mechanism of the reaction. It is likely, though, that initial reaction at the interface of Bi_2S_3 and PbS grains will be to form galenobismutite, the 1 : 1 phase, and that further reaction will then take place between this phase and the excess Bi_2S_3 present.

In this context it is of interest to note that one of the common types of disorder found in these solid state reacted samples of phase V compounds not reported before are bands of type . . . AAAA . . . or . . . BBBB . . . of varying width inserted into the normal phase V sequence. The sequence . . . AAAA . . . has the same stoichiometry as Bi_2S_3, $MS_{1.500}$, while the sequence of layers . . . BBBB . . . has the same stoichiometry as galenobismutite, $MS_{1.333}$. Thus, insertion of extra *A* sequences corresponds to oxidation, that is intergrowth of extra Bi_2S_3 in the phase V matrix while extra *B* sequences corresponds to reduction, that is, intergrowth of galenobismutite into the phase V matrix. We may either have, therefore, an indication of the situation where the phase V compound is unmixing to the end components Bi_2S_3 and galenobismutite, or else an indication of how such end members gradually transform to the phase V structures. Because there is more Bi_2S_3 present in the preparations there should be more of the . . . AAAA . . . sequences than . . . BBBB . . . sequences, and this is exactly the case, with a 13-to-4 ratio found in the results.

The concept of the phase V compounds as ordered or disordered intergrowths of Bi_2S_3 and galenobismutite fits in with a number of trends found in materials which utilize intergrowth as a means of accomodating a variation in anion-to-cation ratio. For example, the TiO_2–Ga_2O_3 system has a low-temperature intermediate phase Ti Ga_2O_5 present at all temperatures. At high temperatures, however, a series of intergrowth phases form between TiO_2 and Ti Ga_2O_5 precisely analogous to the phase V group studied here (*15*). The situation that two compatible crystal structures may intergrow at high temperatures may therefore be widespread but not recognized because of the difficulty of carrying out high-temperature experiments and of characterizing the intergrowth phases themselves when they are disordered.

Further work on the mechanism of formation of the phase V group of compounds and how they unmix at low temperature would be of interest in this general context and is the subject of continuing study.

Acknowledgment

A.C.W. is indebted to the SERC for financial support.

References

1. J. S. Anderson and B. G. Hyde, *J. Solid State Chem.* **9,** 92 (1974).
2. H. J. van Hook, *Econ. Geol.* **55,** 759 (1960).
3. J. R. Craig, *Miner. Deposita* **1,** 278 (1967).
4. B. Salanci and G. Moh, *Neues Jahrb. Mineral Abh.* **112,** 63 (1969).

5. Y. U. TAKÉUCHI, J. TAKAGI, AND T. YAMANAKA, *Z. Kristallogr.* **140,** 9 (1974).
6. Y. U. TAKÉUCHI, T. OZAWA, AND J. TAKAGI, *Z. Kristallogr.* **150,** 75 (1979).
7. D. COLAÏTIS, D. VAN DYCK, AND S. AMELINCKX, *Phys. Status Solidi A* **68,** 419 (1981).
8. D. VAN DYKE, D. COLAÏTIS, AND S. AMELINCKX, *Phys. Status Solidi A* **68,** 385 (1981).
9. R. J. D. TILLEY AND A. C. WRIGHT, *Chem. Scr.* **19,** 18 (1982).
10. E. MAKOVICKY AND S. KARUP-MØLLER, *Neues Jahrb. Mineral. Abh.* **130,** 264 (1977); **131,** 56 (1977).
11. A. G. NORD, *Univ. Stockholm Inorg. Phys. Chem. DIS* **33** (1969).
12. P. E. WERNER, *Ark. Kemi* **31,** 513 (1969).
13. L. G. BERRY, *Amer. Mineral.* **25,** 726 (1940).
14. H. E. SWANSON, NBS Circular 539, Vol. IV, p. 23 (1953).
15. S. KAMIYA AND R. J. D. TILLEY, *J. Solid State Chem.* **22,** 205 (1977).
16. Y. IITAKA AND W. NOWACKI, *Acta Crystallogr.* **15,** 691 (1962).
17. V. KUPČIK AND L. VESELA-NOVAKOVA, *Tschermaks Mineral. Petrogr. Mitt.* **14,** 55, (1970).